

Sonia Casamento,¹ BSc.(Hons.); Ben Kwok,² BSc.(Hons.); Claude Roux,¹ Ph.D.;
Michael Dawson,¹ Ph.D.; and Philip Doble,¹ Ph.D.

Optimization of the Separation of Organic Explosives by Capillary Electrophoresis with Artificial Neural Networks

ABSTRACT: The separation of 12 explosives by capillary electrophoresis was optimized with the aid of artificial neural networks (ANNs). The selectivity of the separation was manipulated by varying the concentration of sodium dodecyl sulfate (SDS) and the pH of the electrolyte, while maintaining the buffer concentration at 10 mM borate. The concentration of SDS and the electrolyte pH were used as input variables and the mobility of the explosives were used as output variables for the ANN. In total, eight experiments were performed based on a factorial design to train a variety of artificial neural network architectures. A further three experiments were required to train ANN architectures to adequately model the experimental space. A product resolution response surface was constructed based on the predicted mobilities of the best performing ANN. This response surface pointed to two optima; pH 9.0–9.1 and 60–65 mM SDS, and pH 8.4–8.6 and 50–60 mM SDS. Separation of all 12 explosives was achieved at the second optimum.

The separation was further improved by changing the capillary to an extended cell detection window and reducing the diameter of the capillary from 75 μm to 50 μm . This provided a more efficient separation without compromising detection sensitivity.

KEYWORDS: forensic science, capillary electrophoresis, explosives, artificial neural network, optimization

The need for forensic laboratories to detect and identify explosive materials arises from two issues: trace analysis of explosive compounds on a suspect person or object, and the analysis of post explosion residues. After an explosion, the majority of the products formed from the explosive materials are generally simple gaseous oxides, which are not useful for forensic analysis. The detection and identification are therefore most often limited to any unreacted original explosive or possibly condensed products.

The techniques most commonly used for the analysis of explosives include thin layer chromatography (TLC), high performance liquid chromatography (HPLC), gas chromatography (GC) and infra-red spectroscopy (IRS). TLC has the advantages of low cost, low solvent consumption and rapid analysis time. However, the sensitivity of detection is often too low for the trace analysis of some explosives (1). TLC is now generally used as a part of clean up procedures or as a screening test (2).

Gas chromatography has high resolution and the ability to use a variety of detection methods, including chemiluminescence, mass spectrometry, electron capture and flame ionization. This detection versatility is offset by the instability of explosives at high temperatures. Therefore precise operating conditions are required.

HPLC is currently considered the method of choice. This is primarily because the analysis can be conducted at room temperature, resolving the problem of thermal instability encountered in GC. HPLC also requires fewer sample clean up procedures than GC.

However, HPLC requires much greater injection volumes in comparison to GC (2). Furthermore, HPLC has relatively high running costs and a large amount of solvent use.

Capillary electrophoresis in the micellar electrokinetic chromatographic (MEKC) mode can be used as an alternative technique for the analysis of explosives. MEKC involves the addition of a surfactant to the electrolyte, which forms micelles that have a hydrophobic interior and therefore allows separation of neutral molecules. Some advantages of MEKC are high efficiency separations with relatively short analysis times (3,4), less reagent use and very small sample sizes, usually in the order of nanolitres. However, MEKC has been found to give less reproducible migration times and peak areas than HPLC (5). MEKC has good mass sensitivity but lacks in concentration sensitivity in comparison to other methods.

Northrop et al. (6) investigated an MEKC separation of 26 organic gunshot and explosive compounds by evaluating factors such as electrolyte pH, micellar concentration, capillary diameter, and injection time. The authors were unable to separate all of the explosives with two pairs co-migrating under the optimized conditions. Other studies of sampling, quantitation, and detection methods have been reported for the analysis of explosives based on the conditions developed by Northrop et al. (7–11). These separations were optimized by a univariate approach in which one electrolyte variable was changed while the others were kept constant. Although this method often eventually arrives at suitable separation conditions, a large number of experiments are required to arrive at an optimum. Furthermore, it is impossible to be sure that the separation is at the true optimum.

A method to reduce the number of experiments is to employ a multivariate approach in which the variables are changed according to an experimental design that encompasses the useful extremes of

¹ Centre for Forensic Science, Department of Chemistry, Materials and Forensic Science University of Technology, Sydney, PO Box 123, Broadway, NSW, Australia, 2007.

² Australian Federal Police, GPO Box 401, Canberra, ACT, Australia, 2601.
Received 20 Jan. 2003; and in revised form 26 April 2003; accepted 26 April 2003; published 4 Aug. 2003.

the electrolytes' variables. The response surface may then be interpolated with a suitable mathematical technique. Once the chromatographic response surface has been calculated the choice of the optimum is straight forward. Artificial neural networks (ANNs) provide a means to interpolate the chromatographic response surface.

An ANN is loosely modeled on the architecture of the brain and learns by example (12). Representative data are collected and delivered to the ANN, where training algorithms are called to learn the structure of the data. An ANN usually consists of neurons arranged in a three layered topology consisting of an input layer, a hidden layer and an output layer. The hidden and output neurons are all connected to the preceding layer. When the ANN is executed it attempts to learn the structure of the data by a feed forward iterative process that continually adjusts the weights of each of the neurons in the hidden and output layer to minimize the error of the response surface. Each iteration is known as an epoch. After a suitable number of epochs the neural network will arrive at a minimum error which may be used to interpolate the response surface.

In this investigation, we report the optimization of the separation of 12 common explosives by MEKC with the aid of an ANN. The pH of the electrolyte and the surfactant concentration were used as the input variables of the ANN, while the output was the mobility of the explosives. In total, eight experiments were required to accurately model the response surface, which allowed the identification of an optimum in which all 12 explosives were separated in under 11 min.

Materials and Methods

Instrumentation

Experiments were conducted on an Agilent Chemstation Capillary Electrophoresis System (Agilent Technologies, Germany). Analyses were carried out at a temperature of 25°C with an applied voltage of 20 kV (+ polarity). A 75.0 μm ID fused-silica capillary (Polymicro Technologies) was employed for the initial experiments, having an effective length of 60.0 cm and a total length of 68.5 cm. Sample introduction was by hydrodynamic pressure injection of 30 mbar for a time of 3 s. Absorbance was measured using a UV diode array detector at wavelengths of 200 nm, 214 nm, 229 nm and 254 nm. Further experiments were performed with a 50 μm ID fused-silica bubble cell capillary (Polymicro Technologies). This capillary had a total length of 64.5 cm and an effective length of 56.0 cm. The injection time was decreased to 2 s and a further detection wavelength at 195 nm was employed.

Reagents

The explosives were purchased from either Radian International or Alltech as either a solid, liquid or standard solution in acetonitrile. Sodium tetraborate (decahydrate), boric acid, sodium dodecyl sulfate (SDS), acetonitrile (HPLC grade) and sodium hydroxide were obtained from Sigma. All water used was 18 M Ω Milli-Q water, generated by the Millipore system.

Twelve explosives were chosen for the analysis and a summary of each is given in Table 1. These explosives were primarily selected due to their availability and provided a range of both high and low explosives.

Stock solutions of 100 mM SDS and 100 mM sodium tetraborate were prepared with Milli-Q water. All analyses utilized a running buffer containing 10 mM borate with the appropriate SDS concentration and pH. The pH was adjusted higher by addition of carbonate free NaOH solution. To adjust the pH to a lower value, 100 mM boric acid was combined with 100 mM sodium tetraborate to give

TABLE 1—*Abbreviation and classification of selected explosives.*

Explosive	Abbreviation	Classification and Use
2,3-Dinitrotoluene	2,3-DNT	Low explosive, propellant, nitroaromatic, constituent in smokeless powder
2,4-Dinitrotoluene	2,4-DNT	
2,6-Dinitrotoluene	2,6-DNT	
3,4-Dinitrotoluene	3,4-DNT	Low explosive, nitroaromatic
2-Nitrotoluene	2-NT	
3-Nitrotoluene	3-NT	
4-Nitrotoluene	4-NT	
Octahydro-1,3,5,7-tetranitro-1,3,5,7-tetrazocine	HMX	Organic high explosive, nitramine, military
Hexahydro-1,3,5-trinitro-1,3,5-triazine	RDX	
2,4,6,N-Tetranitro-N-methylaniline	Tetryl	Organic high explosive, nitroaromatic, military
2,4,6-Trinitrotoluene	TNT	Organic high explosive, nitroaromatic, military
Pentaerythritol Tetranitrate	PETN	Organic high explosive, nitrate ester, military

approximately a 10 mM borate concentration. Each buffer was degassed and filtered using a 0.22 μm nylon filter.

Standards of 1000 ppm were prepared using HPLC grade acetonitrile. These were stored at 4°C and allowed to adjust to room temperature before use. The standards were diluted to 10 ppm with a 50% solution of the running buffer.

Mobility Calculations

The effective mobility for each of the explosives was calculated by establishing the migration time of each analyte and the migration time of the electroosmotic flow (EOF). The peak apex determined the analyte migration times. The start of the EOF peak was used as the migration time for the electroosmotic flow.

Artificial Neural Networks

The software used for establishing networks was Trajan Neural Networks, Version 4.0 (Trajan Software Ltd.). The electrolyte pH and SDS concentration were used as the inputs, and the mobility of each of the explosives was used as the outputs. ANN architectures to model the chromatographic response were constructed using an automated heuristic process in which the number of nodes in the hidden layer was varied, and suitable architectures chosen when the training and verification errors were at a minimum, and similar in magnitude. The mobilities of each of the explosives were then predicted throughout the experimental space by inputting a grid pattern of SDS concentration in the range of 10 mM to 80 mM at increments of 5 mM, and pH in the range of 8.0 to 10.4 at increments of 0.2 pH units.

Resolution Response Surface

The product resolution was determined by multiplying the peak pair resolutions calculated from the explosive mobilities predicted by the ANN. For this calculation, it was assumed that the peak widths were constant for each experiment. Therefore, the peak pair resolution calculation was reduced to the difference between the mobility of each of the adjacent peaks. The product resolution was chosen as it gives a simple measure of the overall resolution of the separation, with the largest value representing the greatest spread of the peaks.

Results and Discussion

Optimization

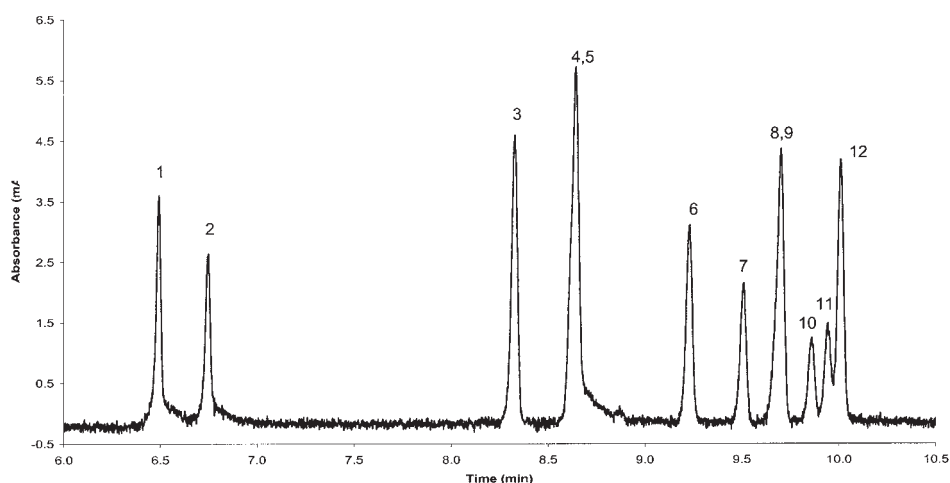
Preliminary experiments indicated that the selectivity of the separation was controlled by the pH and the SDS concentration in the buffer. The concentration of the borate buffer had little effect on the selectivity of the separation and was therefore kept constant at 10 mM for all optimization experiments. Five initial experiments based on a factorial design were performed (Table 2). The concentration range of the SDS was 10 mM to 80 mM, and the pH range was from 8.2 to 10.2 which is the useful buffering capacity of borate (pKa 9.24).

In each of experiments 1, 3, and 5, two co-eluting pairs occurred. For Experiment 1 (Fig. 1(i)) and Experiment 3 (Fig. 1 (iii)) these pairs were PETN/Tetryl and 2,3-DNT/2-NT. The co-eluting pairs for Experiment 5 (Fig. 1(v)) were 2,3-DNT/2-NT, and 3-NT/3,4-

TABLE 2—SDS concentration, pH and the co-eluting analytes of experiments performed.

Experiment	pH	[SDS] (mM)	Co-eluting Analytes
1	9.21	45	(PETN/Tetryl), (2,3-DNT/2-NT)
2	8.24	10	(TNT/PETN), (2,6-DNT/2-NT), (2,3-DNT/4-NT/3-NT)
3	8.24	80	(PETN/Tetryl), (2,3-DNT/2-NT)
4	10.17	10	(HMX/RDX), (TNT/PETN), (Tetryl/2,4-DNT), (2,6-DNT/2-NT/2,3-DNT/4-NT/3-NT), (3,4-DNT)
5	10.14	80	(2,3-DNT/2-NT), (3-NT/3,4-DNT)
6	9.03	17	(PETN/Tetryl), (4-NT/3-NT)
7	9.27	60	(PETN/Tetryl), (2,3-DNT/2-NT)
8	9.28	30	(PETN/Tetryl), (2,3-DNT/2-NT)
9	9.01	65	(PETN/Tetryl), (2,3-DNT/2-NT)
10	8.5	55	none

Figure 1 (i)



(ii)

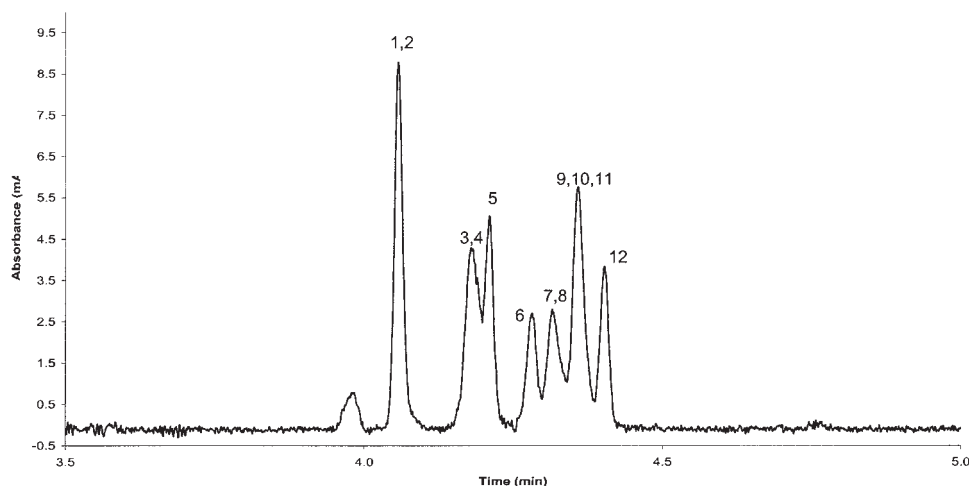


FIG. 1—Electropherograms of Experiments 1–8 (12 explosives at 10 ppm)—75 μ m ID capillary, total length 68.5 cm, effective length 60.0 cm. 30 mbar for 2s injection, +20 kV applied voltage, 25°C temperature, 195 nm detection wavelength. (1) HMX (2) RDX (3) TNT (4) PETN (5) Tetryl (6) 2,4-DNT (7) 2,6-DNT (8) 2-NT, (9) 2,3-DNT (10) 4-NT (11) 3-NT (12) 3,4-DNT. (i) Experiment 1. SDS 45 mM, pH 9.21, borate 10 mM. (ii) Experiment 2. SDS 10 mM, pH 8.24, borate 10 mM. (iii) Experiment 3. SDS 80 mM, pH 8.24, borate 10 mM. (iv) Experiment 4. SDS 10 mM, pH 10.17, borate 10 mM. (v) Experiment 5. SDS 80 mM, pH 10.14, borate 10 mM. (vi) Experiment 6. SDS 17 mM, pH 9.03, borate 10 mM. (vii) Experiment 7. SDS 60 mM, pH 9.27, borate 10 mM. (viii) Experiment 8. SDS 30 mM, pH 9.28, borate 10 mM.

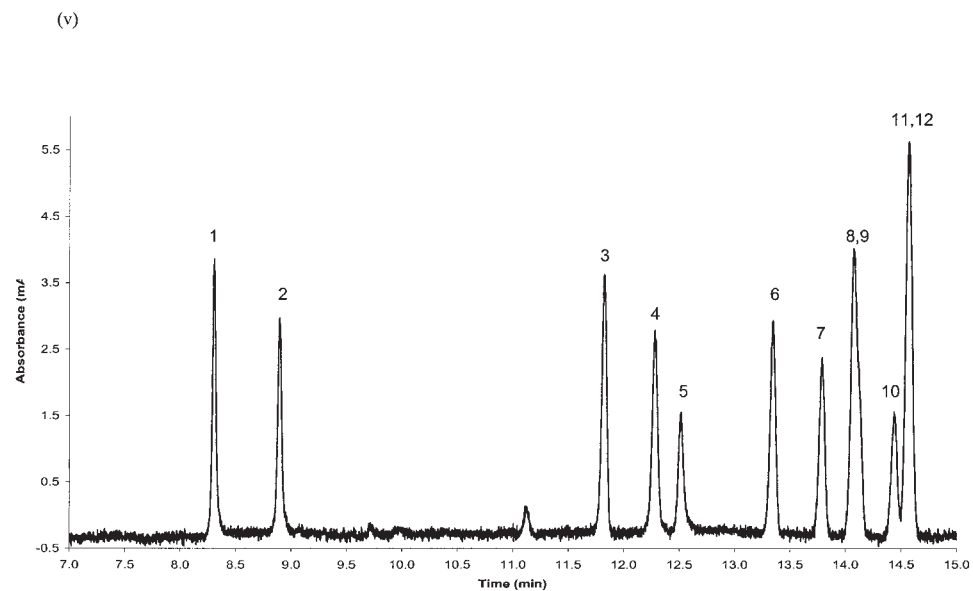
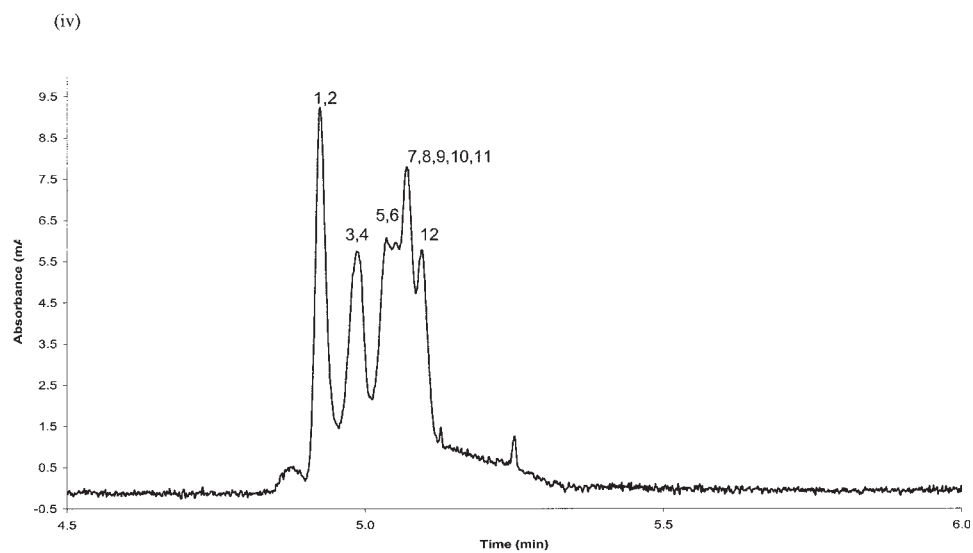
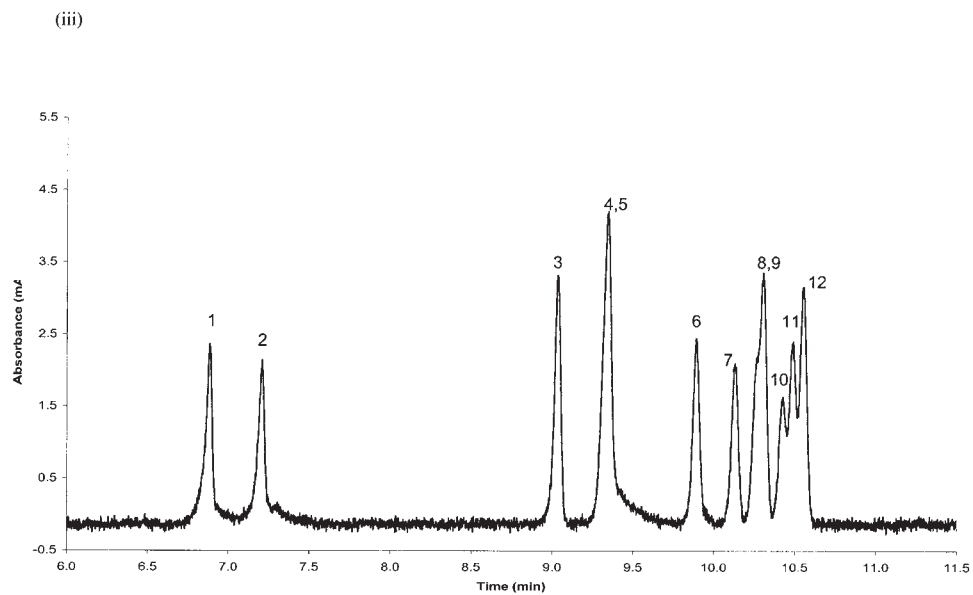


FIG. 1—(continued)

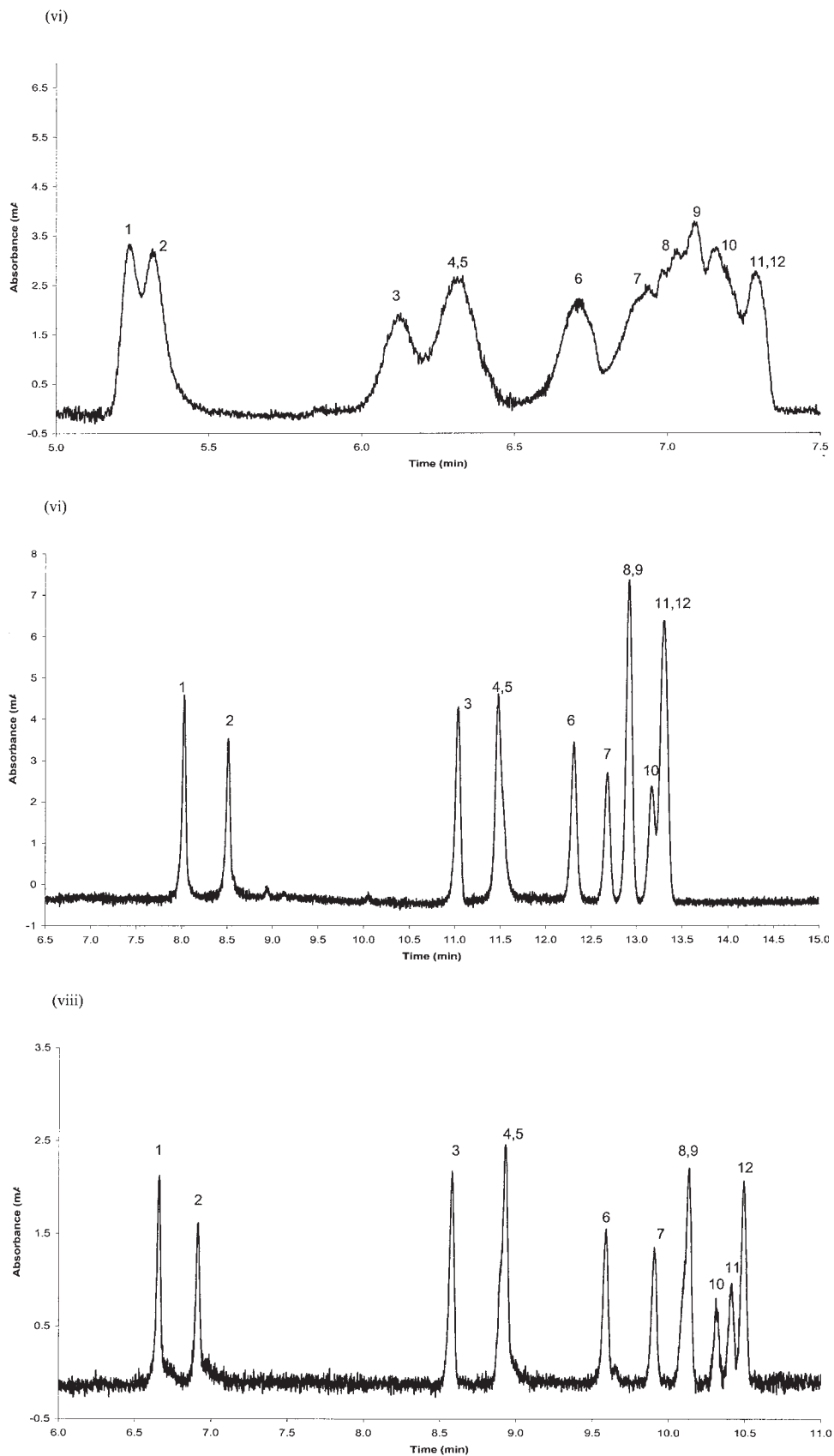


FIG. 1—(continued)

TABLE 3—Average effective mobility ($\text{cm}^2\text{V}^{-1}\text{min}^{-1} \times 10^{-3}$) for Experiments 1–8.

Experiment	1	2	3	4	5	6	7	8
HMX	-9.14	-1.44	-14.32	-0.73	-13.18	-4.94	-13.31	-8.16
RDX	-10.34	-1.44	-15.66	-0.73	-14.78	-5.51	-14.79	-9.28
TNT	-16.14	-2.94	-21.44	-1.26	-20.44	-10.57	-20.29	-15.07
PETN	-17.04	-2.93	-22.20	-1.26	-21.35	-11.60	-21.01	-16.00
Tetryl	-17.04	-3.27	-22.20	-1.93	-21.08	-11.60	-21.01	-16.00
2,4-DNT	-18.55	-4.09	-23.42	-1.93	-22.39	-14.54	-22.21	-17.59
2,6-DNT	-19.21	-4.48	-23.92	-1.93	-22.88	-14.72	-22.70	-18.28
2-NT	-19.64	-4.48	-24.27	-1.93	-23.18	-14.94	-23.00	-18.73
2,3-DNT	-19.64	-4.93	-24.27	-1.93	-23.18	-15.17	-23.00	-18.73
4-NT	-19.98	-4.93	-24.50	-1.93	-23.53	-15.46	-23.30	-19.08
3-NT	-20.16	-4.93	-24.62	-1.93	-23.66	-15.46	-23.45	-19.28
3,4-DNT	-20.29	-5.41	-24.75	-1.93	-23.66	-15.96	-23.45	-19.43

DNT while PETN and Tetryl were fully resolved. In Experiment 2 (Fig. 1(ii)) and Experiment 4 (Fig. 1(iv)) all the analytes eluted within 6 min. Only seven peaks were present in Experiment 2, while in Experiment 4, only three major peaks were observed. This is not surprising as both these experiments had the lower SDS concentration of 10 mM, therefore the least resolving power.

The mobility for each analyte was calculated under each of the first five experimental conditions and the average mobility for each analyte, given in Table 3, was obtained. A number of ANN architectures were constructed without verification points as the number of experiments was limited. This pointed to an optimum present at pH 9.03 and SDS at 17 mM. This experiment resulted in poor separation of the 12 analytes as shown in Fig. 1 (vi). This poor performance was most likely due to overlearning of the ANN. Although the model had very low error, it had poor predictive capabilities.

Two more experiments were performed to acquire more data to train the network. Experiment 7 (Fig. 1(vii)) consisted of a buffer of pH 9.27 and SDS concentration of 60 mM, and Experiment 8 (Fig. 1(viii)) consisted of a 30 mM SDS concentration and pH of 9.28 (Table 2). These two points were chosen because inspection of the preceding electropherograms indicated that the optimum was somewhere near the middle of the chosen experimental space. From these eight experiments, different models were constructed by varying the experiments used as training and verification inputs. The model that minimized the training and verification error values was selected to construct the product resolution response surface (Fig. 2).

From this product resolution response surface, two optima were evident. The first optimum was between an SDS concentration of approximately 60 mM to 65 mM and a pH of 9.0 to 9.1. The second optimum showed a high product resolution within a SDS concentration 50 mM to 60 mM and pH range of 8.4–8.6. The latter electrolyte composition resulted in complete separation of all 12 explosives and is shown in Fig. 3 (i). The separation was further improved by transferring the separation to a 50 μm ID capillary with an extended optical pathlength of 75 μm . This resulted in improved resolution of all of the explosives without compromising the detection sensitivity and is shown in Fig. 3 (ii).

Analytical Performance

Linear Range

The linear range for each of the explosives was calculated over the range of 1 to 40 ppm based upon normalized peak area (area/migration time), peak area and peak height. Triplicate measurements of seven points at 1, 2, 5, 10, 20, 30 and 40 ppm were taken

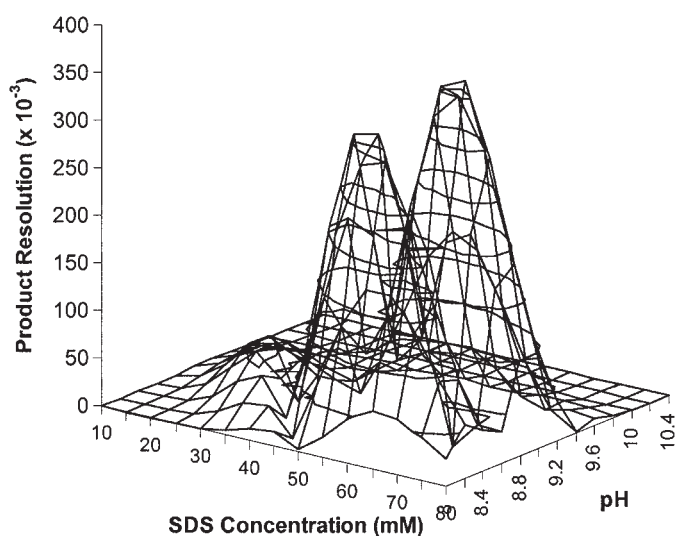


FIG. 2—ANN predicted product resolution response surface.

and the average was used for construction of the analyte calibration curve. The correlation coefficients are given in Table 4. There was no significant difference between the normalized peak area and peak area with correlation coefficients ranging from 0.9925 to 0.9996, indicating a high degree of linearity for all explosives. The peak height gave considerably worse correlation coefficients for the majority of the analytes, ranging from 0.8576–0.9983. Therefore, only peak areas should be used for quantitation.

Detection Limits

The detection limit was approximately 1 ppm (shown in Fig. 4) for all of the explosives, based on a signal to noise ratio of 3:1. The calculated injection volume was 1.4 nL, corresponding to a mass detection limit of approximately 1.4 pg.

Repeatability

The repeatability of the peak areas, migration times, and mobility was measured by triplicate injections of the explosive standards at 5, 10, and 20 ppm. The peak area repeatability was of the order of 1 to 4% RSD (relative standard deviation), the migration time repeatability ranged from 1–2%, and the mobility repeatability was less than 1% RSD. Therefore mobility is clearly a better indicator

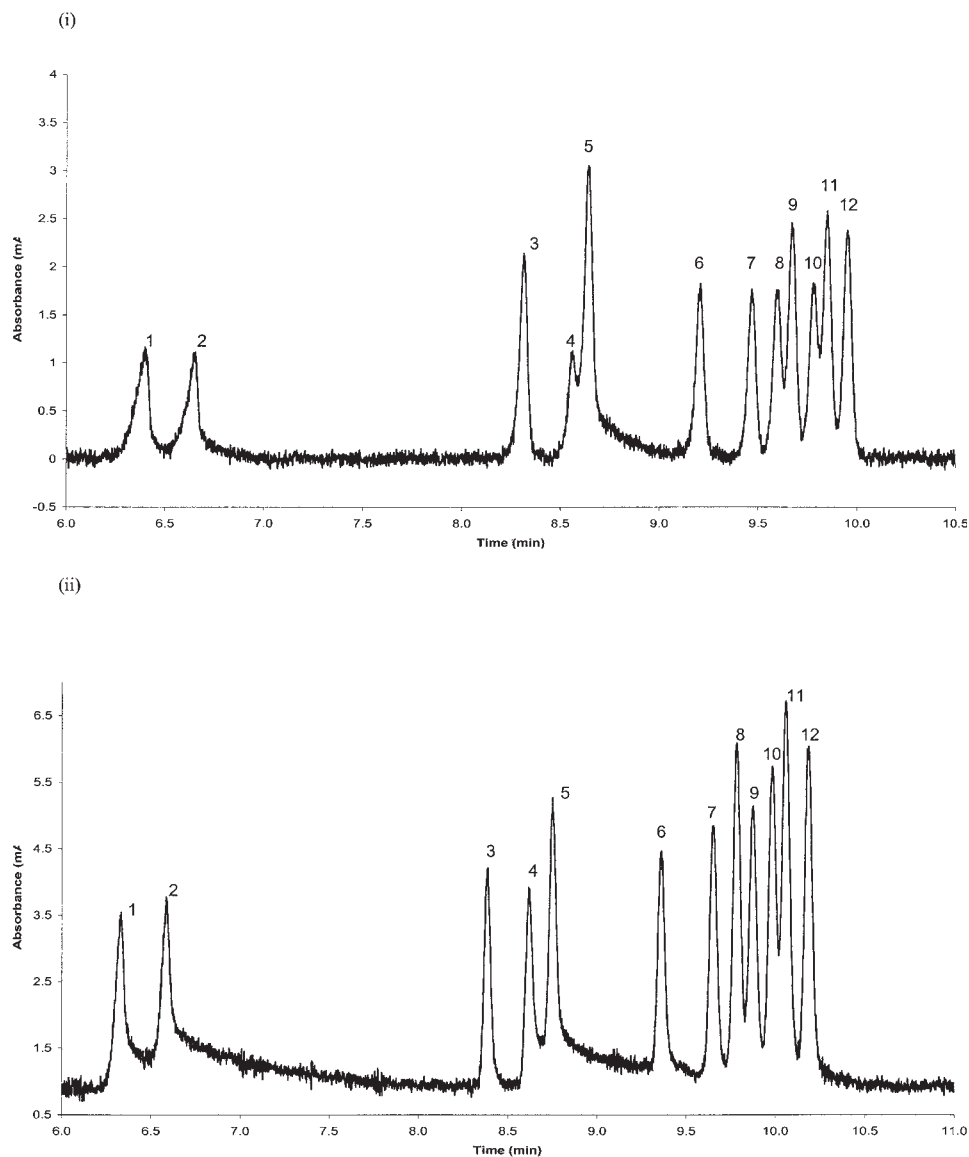


FIG. 3—Electropherogram of Experiment 10 (12 explosives at 10 ppm). SDS 55 mM, pH of 8, borate 10 mM. (1) HMX (2) RDX (3) TNT (4) PETN (5) Tetryl (6) 2,4-DNT (7) 2,6-DNT (8) 2-NT, (9) 2,3-DNT (10) 4-NT (11) 3-NT (12) 3,4-DNT. (i) 75 μm ID capillary, total length 68.5 cm, effective length 60.0 cm. 30 mbar for 3s injection, +20 kV applied voltage, 25°C temperature, 214 nm detection wavelength. (ii) 50 μm ID bubble cell capillary (detection window 75 μm ID), total length 64.5 cm, effective length 56.0 cm. 30 mbar for 2s injection, +20 kV applied voltage, 25°C temperature, 195 nm detection wavelength.

TABLE 4—Correlation coefficients for calibration curves over 1–40 ppm.

Explosive	Normalized Peak Area (mAU)	Peak Area (mAU.s)	Peak Height (mAU)
HMX	0.9974	0.9974	0.8848
RDX	0.9955	0.9957	0.8576
TNT	0.9980	0.9984	0.9755
PETN	0.9982	0.9983	0.9879
Tetryl	0.9987	0.9989	0.9862
2,4-DNT	0.9997	0.9996	0.9929
2,6-DNT	0.9993	0.9996	0.9955
2-NT	0.9930	0.9944	0.9976
2,3-DNT	0.9973	0.9970	0.9862
4-NT	0.9925	0.9940	0.9983
3-NT	0.9936	0.9947	0.9978
3,4-DNT	0.9994	0.9996	0.9967

of explosive identity than migration time. This is not unexpected as mobility measurements are independent of the EOF.

Analysis of EPA Standard

In order to test the method for quantitative accuracy, an EPA standard containing 14 explosives at a known concentration of 10 ppm was separated and quantitated under the optimized separation conditions (Fig. 5). Nine of the fourteen explosives were identified based upon the respective effective mobility of the analytes. The calculated concentrations ranged from 8.4 ppm to 10.3 ppm (Table 5) indicating a high degree of agreement between the calculated and specified concentrations. The nine explosives were HMX, RDX, TNT, tetryl, 2,4-DNT, 2,6-DNT, 2-NT, 3-NT and 4-NT. The other five explosives present in the EPA reference (method 8330) were nitrobenzene, 1,3-dinitrobenzene, 1,3,5-trinitrobenzene, 2-amino-4,6-dinitrotoluene and 4-amino-2,6-dinitrotoluene.

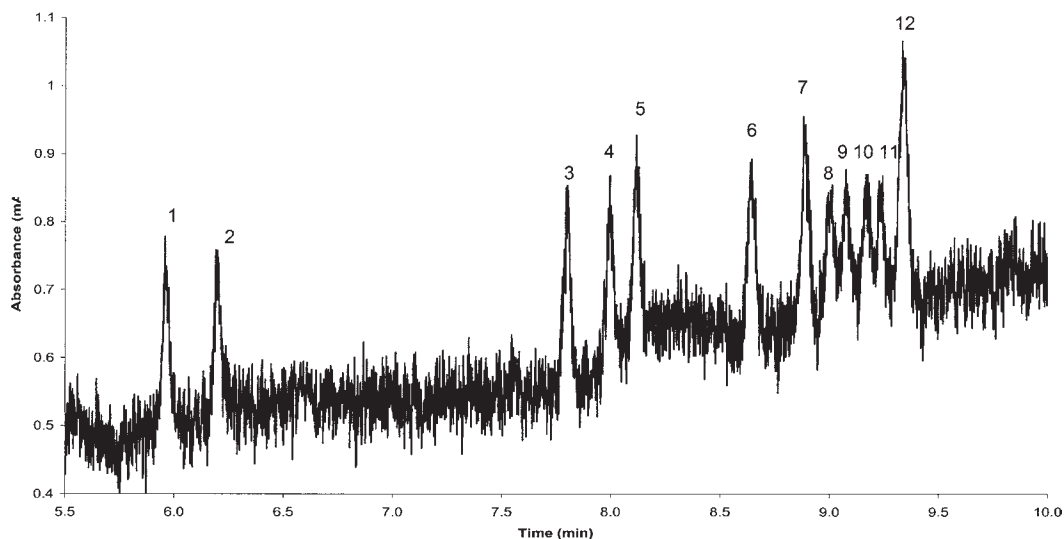


FIG. 4—Electropherogram of 12 explosives at 1 ppm. SDS 55 mM, pH of 8, borate 10 mM. 50 μm ID bubble cell capillary (detection window 75 μm ID), total length 64.5 cm, effective length 56.0 cm. 30 mbar for 2s injection, +20 kV applied voltage, 25°C temperature, 195 nm detection wavelength. (1) HMX (2) RDX (3) TNT (4) PETN (5) Tetryl (6) 2,4-DNT (7) 2,6-DNT (8) 2-NT, (9) 2,3-DNT (10) 4-NT (11) 3-NT (12) 3,4-DNT.

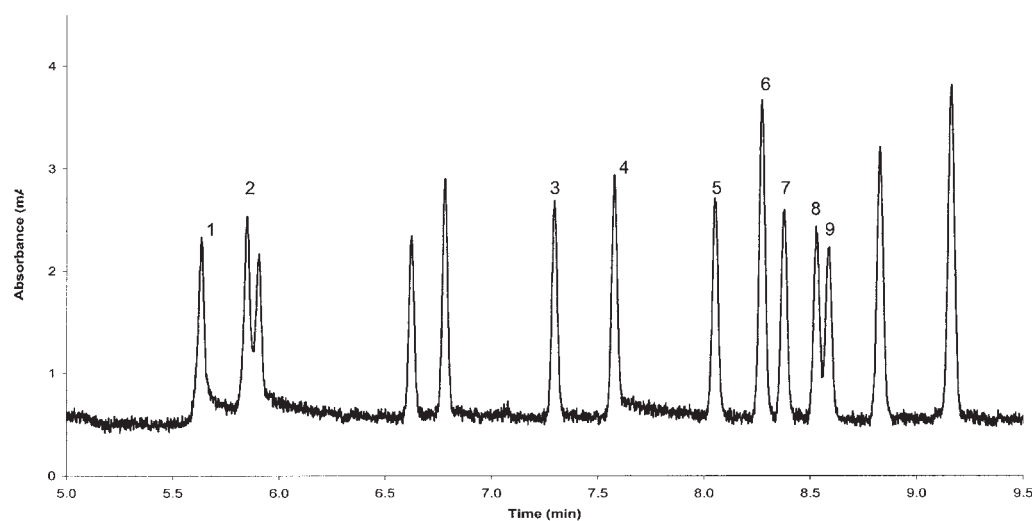


FIG. 5—Electropherogram of EPA standard (method 8830) at 10 ppm. SDS 55 mM, pH of 8, borate 10 mM. 50 μm ID bubble cell capillary (detection window 75 μm ID), total length 64.5 cm, effective length 56.0 cm. 30 mbar for 2s injection, +20 kV applied voltage, 25°C temperature, 195 nm detection wavelength. (1) HMX (2) RDX (3) TNT (4) Tetryl (5) 2,4-DNT (6) 2,6-DNT (7) 2-NT, (8) 4-NT (9) 3-NT.

TABLE 5—Calculated concentrations from calibration curve for 10 ppm EPA standard.

Explosive	HMX	RDX	TNT	Tetryl	2,4-DNT	2,6-DNT	2-NT	4-NT	3-NT
Conc. (ppm)	9.3	10.3	9.5	9.1	9.1	9.3	8.4	8.9	9.1

It should be noted that although these five explosives were not used in the optimization process, the high efficiency of the separation was capable of separating all 14 explosives present in the EPA standard.

Conclusions

An artificial neural network was productively employed for the optimization of the separation of 12 explosives based on a factorial

design consisting of eight experimental points. The SDS concentration and buffer pH from each of the eight experiments were used as the input variables for the ANN, while the effective mobility for each explosive was used as the output variables. The mobility of each explosive was interpolated within the entire experimental space and a product resolution response surface calculated. This approach considerably reduces the amount of experiments and time as the whole experimental response surface can be described from eight experiments. This response surface indicated two regions in

which the product resolutions were at maxima. Both conditions were tested, with the second maximum at 10 mM and SDS concentration of 55 mM resulting in resolution of all 12 explosives. Traditional sequential increments of one variable at a time to build a similar response surface would require an estimated 20 experiments based on 0.5 pH unit and 20 mM SDS increments.

This resolution was further improved without compromising detection sensitivity by changing from a 75 μm i.d. to a 50 μm capillary with an extended optical pathlength of 75 μm .

Detection was linear from 1 ppm to 40 ppm for all 12 explosives. The detection limit for all of the explosives was approximately 1 ppm. The effective mobility, migration time and area repeatability was less than 0.8% RSD, 2.0% RSD and 4.0% RSD respectively.

A 14 explosive EPA (8330) reference standard was used as a test sample. Nine of the fourteen explosives were identified with their concentrations determined from the peak area within at least 16% of the actual values.

References

1. Beveridge AD, editors. Forensic investigation of explosions. London: Taylor and Francis Ltd, 1998
2. Beveridge AD. Development in the detection and identification of explosive residues. *Forensic Sci Rev* 1992;4(1):18–49.
3. Kleibohmer W, Cammann K, Robert J, Mussenbrock E. Determination of explosive residues in soils by micellar electrokinetic capillary chromatography and high-performance liquid chromatography—a Comparative Study. *J Chromatogr A* 1993;638:349–56.
4. Belen'kii BG, Belov YU, Kasalainen GE. High-performance capillary electrophoresis in environmental monitoring. *J Anal Chem* 1996;51(8): 817–34.
5. Belen'kii BG, Belov, YV, Kasalainen GE, Medvedeva MI, Khor ST. High-performance micellar electrokinetic chromatography of explosives. *J Anal Chem* 1998;53(3):329–33
6. Northrop DM, Martire DE, MacCrehan WA. Separation and identification of organic gunshot and explosive constituents by micellar electrokinetic capillary electrophoresis. *Anal Chem* 1991;63(10): 1038–42.
7. Northrop DM, MacCrehan WA. Sample collection, preparation, and quantitation in the micellar electrokinetic capillary electrophoresis of gunshot residues. *J Liquid Chromatogr* 1992;15(6):1041–63.
8. Kennedy S, Caddy B, Douse JMF. Micellar electrokinetic capillary chromatography of high explosives utilising indirect fluorescence detection. *J Chromatogr A* 1996;726(1–2):211–22.
9. Mussenbrock E, Kleibohmer W. Separation strategies for the determination of residues of explosives in soils using micellar electrokinetic capillary chromatography. *J Microcolumn Separations* 1995;7(2): 107–15.
10. Groom CA, Beaudet S, Halasz A, Paquet L, Hawari J. Application of sodium dodecyl sulfate micellar electrokinetic chromatography (SDS MEKC) for the rapid measurement of aqueous phase 2,4,6-trinitrotoluene metabolites in anaerobic sludge: a comparison with LC/MS. *Environ. Sci Technol* 2000;34(11):2330–6.
11. Hilmi A, Luong JHT, Nguyen A. Development of electrokinetic capillary electrophoresis equipped with amperometric detection for analysis of explosive compounds. *Anal Chem* 1999;71(4):873–8.
12. Agatonovic-Kustrin S, Beresford R. Basic concepts of artificial neural network (ANN) modeling and its application in pharmaceutical research. *J Pharm Biomed Anal* 2000;22:717–27.

Additional information and reprint requests:

Philip Doble, Ph.D.

Lecturer

Centre for Forensic Science

Department of Chemistry, Materials and Forensic Science

University of Technology, Sydney

PO Box 123, Broadway, NSW, Australia, 2007